Supporting Information for

Self-oxygenated Wearable Light-Emitting Bandage for Photobiomodulation against Diabetic Wounds

Shenyan Zhang[1], Lingbao Kong[1,3]*, Penghao Ji[2], Minfeng Huo[2]*

[1] Shanghai Engineering Research Center of Ultra-Precision Optical Manufacturing, Department of Optical Science and Engineering, Fudan University, Shanghai 200433, P. R. China

[2] Shanghai Tenth People's Hospital, Shanghai Frontiers Science Center of Nanocatalytic Medicine, The Institute for Biomedical Engineering & Nano Science School of Medicine, School of Medicine, Tongji University, Shanghai, 200072, P. R. China

[3]Yiwu Research Institute, Fudan University, Chengbei Road, Yiwu City 322000, P.R. China

***Corresponding Author, E-mail:** lkong@fudan.edu.cn; mfhuo@tongji.edu.cn

Contents

1. Supplementary method

Characterizations: TEM images were obtained on the JEM-2100F transmission electron microscope (JEOL Ltd, Japan). SEM image was obtained on field-emission Magellan 400 microscope (FEI Company, United States). The temperature of the inflamed joint was recorded using an infrared thermal imaging camera (FLIR A325sc, US). Sequencing was conducted at Novogene Bioinformatics Technology Co., Ltd, China. UV-Vis-NIR absorption spectra were acquired on UV-3600. Confocal laser scanning microscopy (CLSM) images were recorded on FV1000 (Olympus Company, Japan). Absorbance and luminescence profiles were recorded using the microplate reader (Biotek Instruments, Inc., Winooski, VT, USA). Optical power meter CEL-NP2000 (China Education Au-light, China)

The culture of cyanobacteria: Cyanobacteria Synechococcus elongatus PCC 7942 strain was obtained from Freshwater Algae Culture Collection at the Institute of Hydrobiology (FACHB), Chinese Academy of Sciences (CAS). The cells were cultured in Erlenmeyer flask using BG11 culture medium (HB8793, Hopebio Co., Ltd). The culture was continuously irradiated with office lighting on a 12-hour light/dark cycle. The light intensity was adjusted to 6,000 lux by modifying the distance between the light source and the culture. To ensure adequate CO_2 dissolution, the culture was gently shaken twice daily.

Cytotoxicity assay of cyanobacteria: HaCaTs, HUVECs, and HSFs were seeded in the lower chamber of transwell 24-well plate (about 5×10^4 cells per well). After cell attachment, the medium was replaced with fresh medium. Subsequently, 500 μL of fresh medium containing different concentrations of cyanobacteria (5×10^6, 1×10^7, 5×10^7, 1×10^8, and 5×10^8 cells/mL) was added to the upper chamber, which contained 0.4-μm pore-sized filters. The CCK-8 assay was then performed following 24 hours of co-incubation.

Cell culture: HaCaTs, HUVECs, and HSFs were purchased from the cell bank of the Chinese Academy of Sciences (Shanghai). HaCaTs and HSFs were cultured in high-glucose Dulbecco's modified Eagle's medium (DMEM, Gibco) supplemented with 10% fetal bovine serum (FBS, Gibco). HUVECs were cultured in endothelial cell medium (ECM, Gibco). All cells were incubated at 37ºC and 5% CO_2.

The scratch wound-healing assay: Cell scratch was measured using 6-well transwell inserts with 0.4-μm pore-sized filters. Briefly, cells were seeded at a density of 1×10^6 cells per well into the lower chamber and scratched using a sterile p200 pipette tip and washed with PBS to remove unattached cells. Then, the attached cells were treated with cyanobacteria (1×10^8 cells/mL) into the upper chamber in the RL. These cells (HaCaTs, HSFs and HUVECs) were recorded at 0 and 24 hours using optical microscope. The migration rate was evaluated by calculating the ratio of the closed area to the initial wound.

The tube formation assay: For tube formation assay, 1 mL per well of diluted thawed Matrigel (Beyotime, China) was added into the lower chamber of a pre-cooled 6-well plate and incubated for 1 hour at 37°C. Then, HUVECs were seeded with 5×10^5 cells per well into the Matrigel-coated lower chamber and exposed to cyanobacteria (1×10^8 cells/mL) into the upper chamber (0.4-μm pore-sized filters) in the RL for 30 min. After 24h, cells were stained with Calcein-AM, followed by were imaged under a confocal laser scanning microscope and quantified using ImageJ software.

mRNA sequencing: Total RNA was extracted from wound tissue of both groups using an RNeasy Fibrous Tissue Mini Kit. RNA concentration and quality were measured using a NanodropND-1000 spectrophotometer (Gene Company, USA) and a 2100 Bioanalyser (Agilent), respectively. The mRNA was purified using poly-T oligo-attached magnetic beads and fragmented using divalent cations under elevated temperature NEBNext First Strand Synthesis Reaction Buffer (5X). First-strand cDNA was synthesized using a random hexamer primer and M-MuLV Reverse Transcriptase

(RNase H-). Second-strand cDNA synthesis was subsequently performed using DNA Polymerase I and RNase H. Remaining overhangs were converted into blunt ends via exonuclease/polymerase activities. After adenylation of 3' ends of DNA fragments, NEBNext Adaptor with hairpin loop structure was ligated to prepare for hybridization. The products were then enriched and purified (AMPure XP system) to form the final cDNA library and the library quality was assessed on the Agilent Bioanalyzer 2100 system. The clustering of the indexcoded samples was performed on a cBot Cluster Generation System using TruSeq PE Cluster Kit v3-cBot-HS (Illumia) according to the manufacturer's instructions. After cluster generation, the library preparations were sequenced on an Illumina Novaseq platform and 150 bp paired-end reads were generated. The webbased NovoMagic data analysis platform was used for raw data variance modelling and statistical analyses.

2. Supplementary Figures

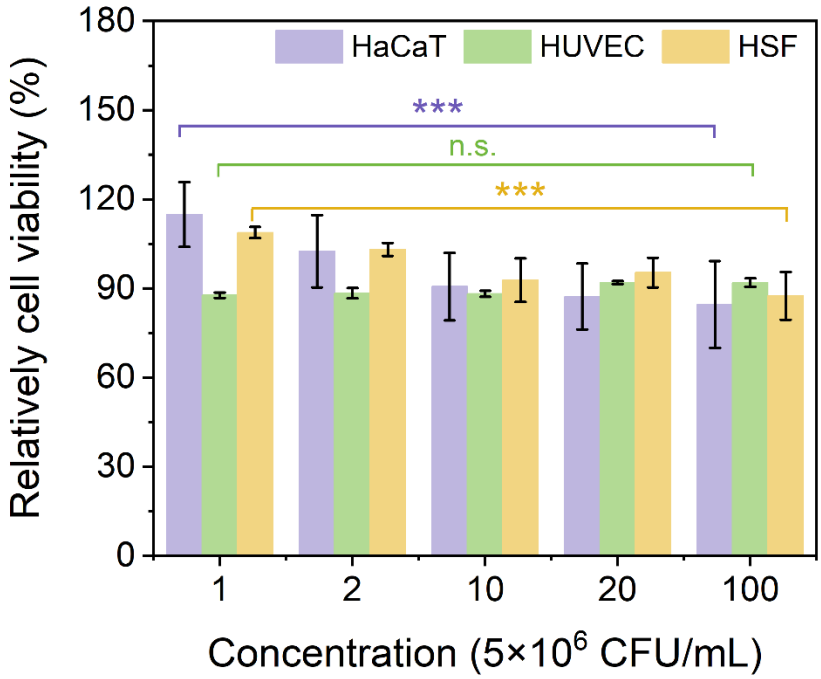

Figure S1. The relative cell viability of HaCaT, HUVEC and HSF cell lines co-incubated with different concentration of cyanobacteria for 24 h. Data are expressed as means ± SD (N = 4). Statistical significances were calculated via ANOVA analysis. n.s. p>0.05, ***P<0. 001.

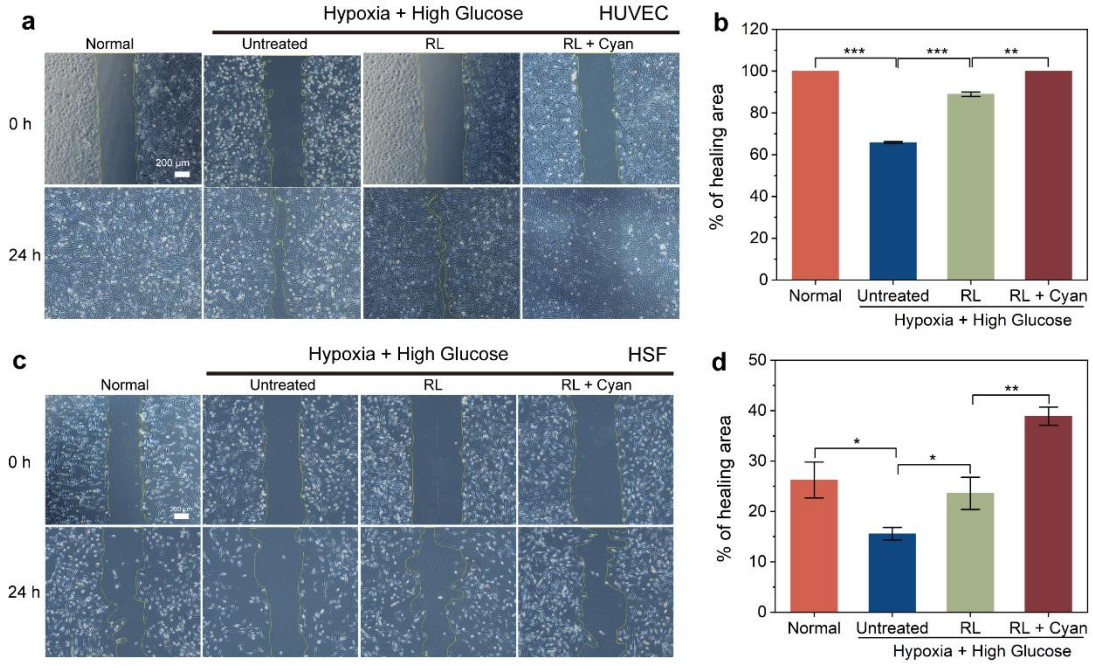

Figure S2. a-d, Representative images and quantification of HUVEC (a-b) and HSF (c-d) migration from different groups. Data are expressed as means ± SD (N = 3). Statistical significances were calculated via Student's t-test. *P<0.05, **P<0.01, ***P<0. 001.

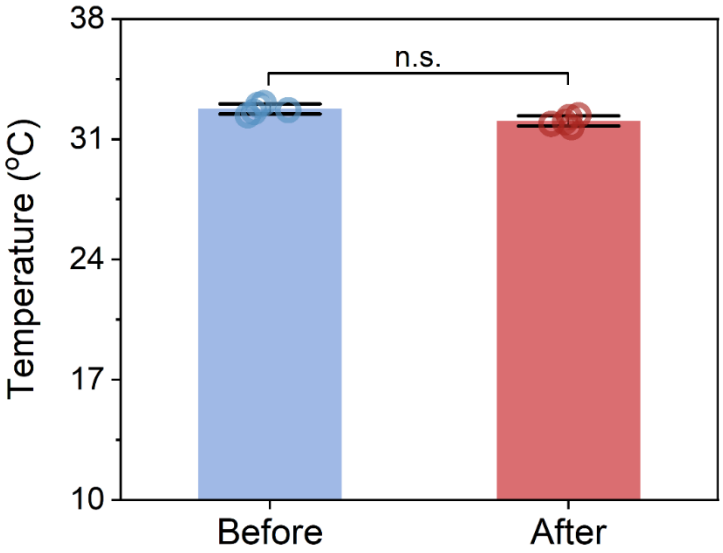

Figure S3. The maximum focal temperature of the forearm of the human subject before and after wearing the LEB. Statistical significances were calculated via Student's t-test. n.s. $p>0.05$

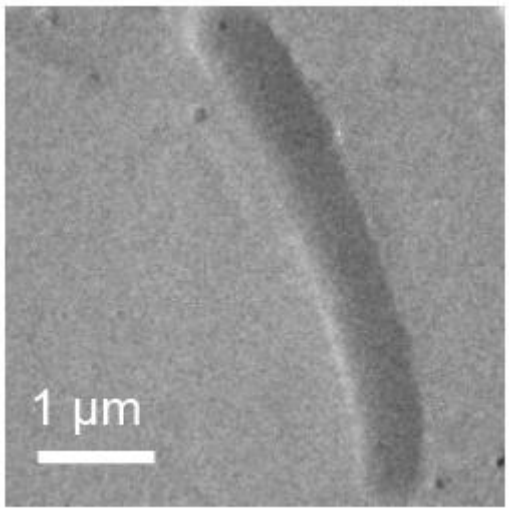

Figure S4. The TEM image of cyanobacteria.

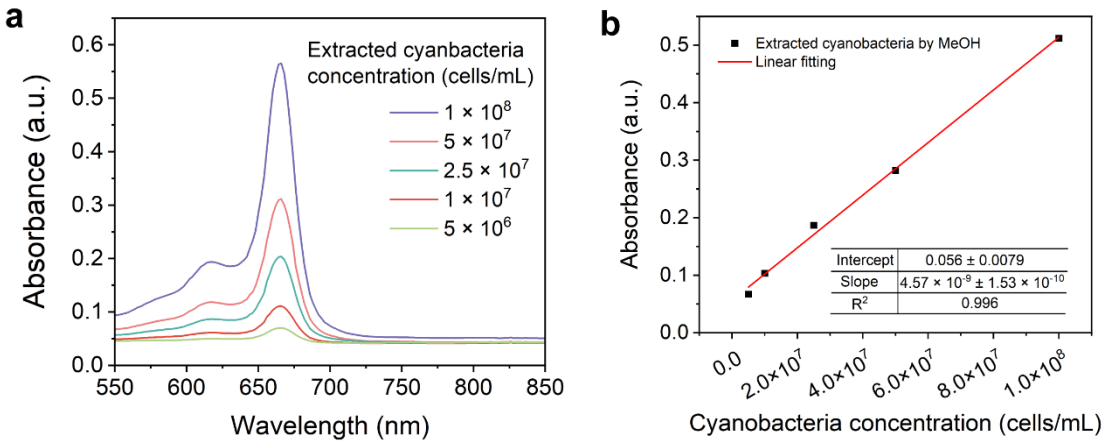

Figure S5. a-b, UV-vis absorbance spectra (a) and corresponding linear fitting at 660 nm (b) of extracted chlorophylls from different concentrations of cyanobacteria by MeOH (90%).

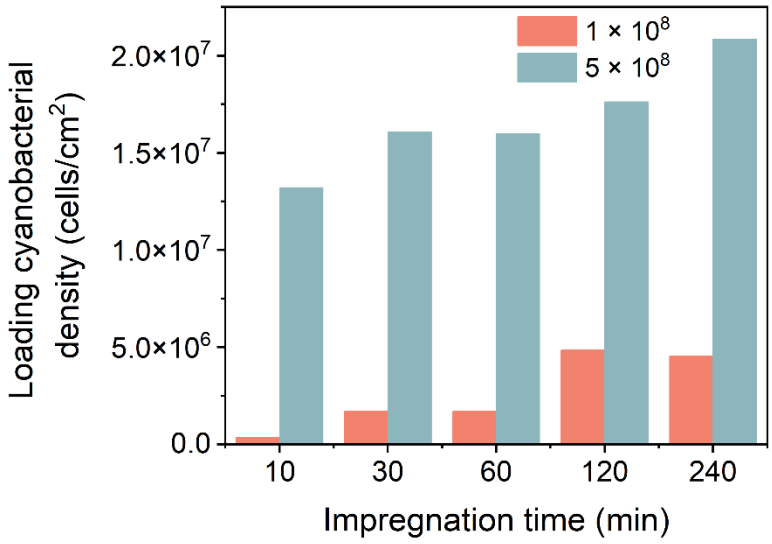

Figure S6. The final cyanobacteria impregnation efficiency of LEB@cyan obtained by immersing different concentrations of cyanobacteria with 1 cm^2 light-emitting fabric at the indicated impregnation time.

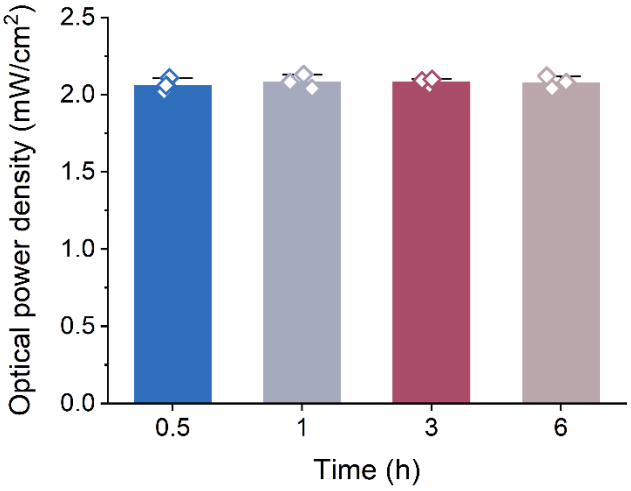

Figure S7. The optical power density of LEB@Cyan on different timepoints (0.5, 1, 3 and 6 h) under continuous operating conditions.

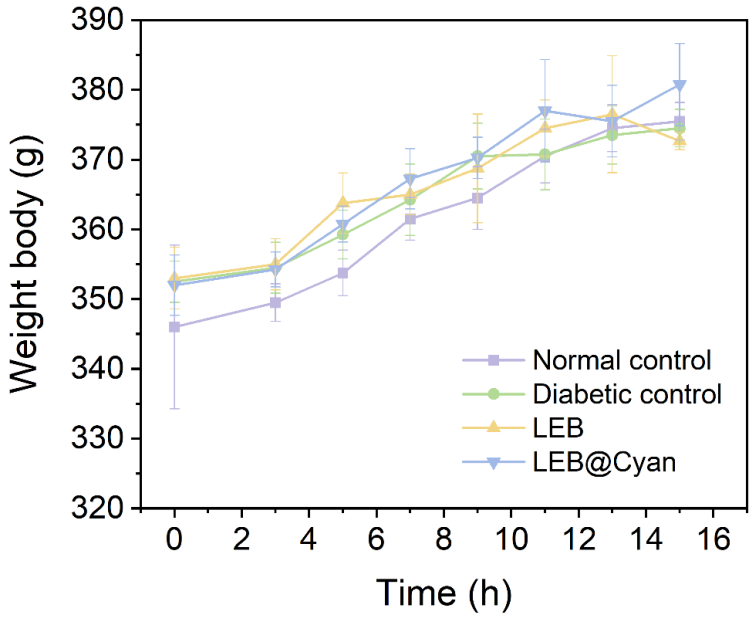

Figure S8. The body weight curves of rats from different groups (N = 5) during the 15-day evaluation period. Data are presented as mean ± s.d.

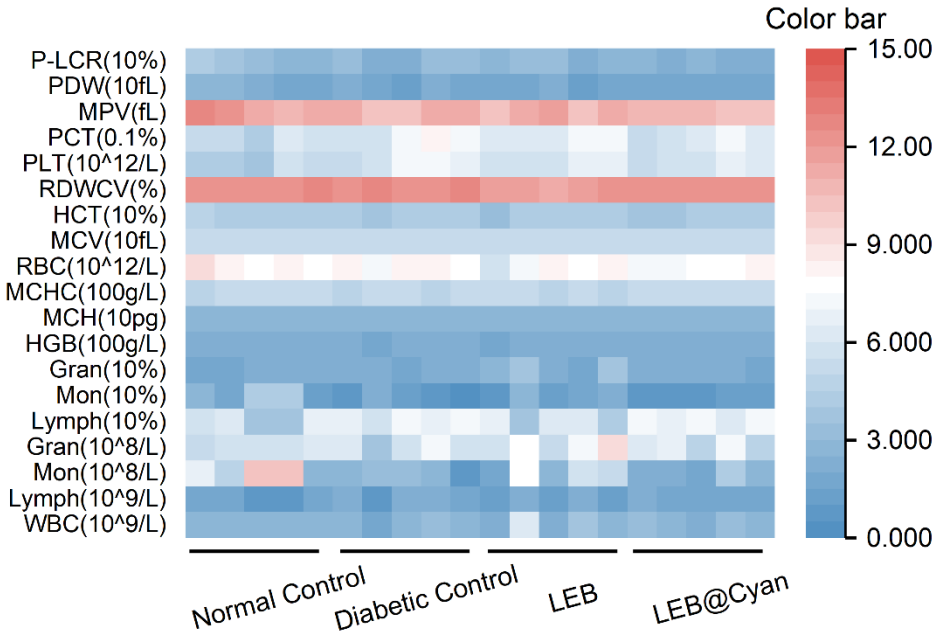

Figure S9. The heat maps of blood routine index of rats from different treatment groups (N = 5) on day 15.

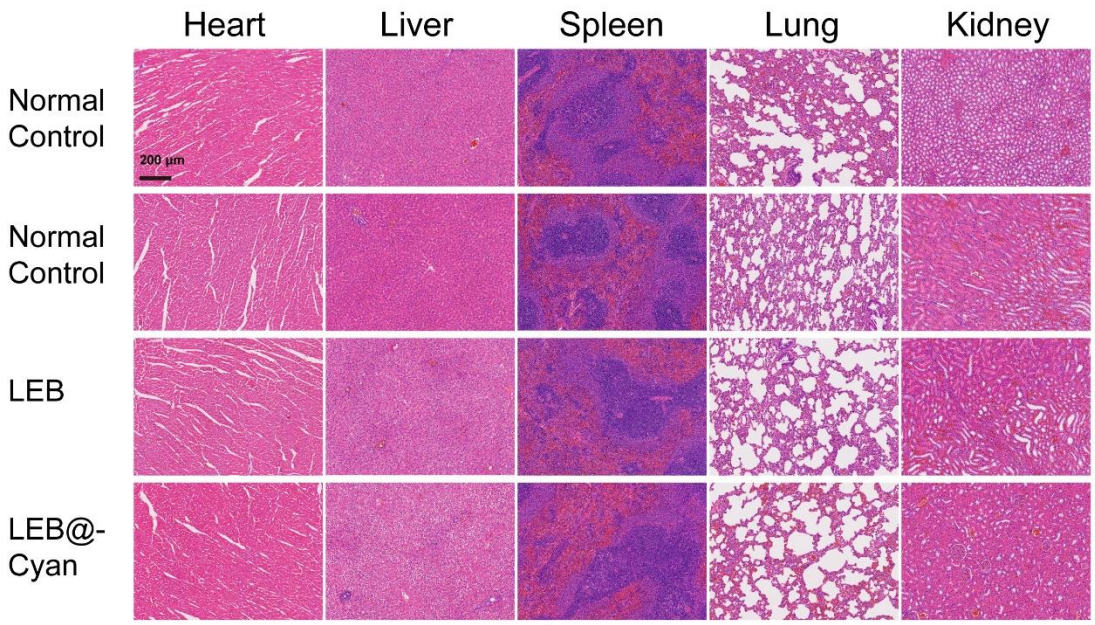

Figure S10. H&E-stained histological images of the heart, liver, spleen, lung, and kidneys of rats from different groups on day 15.

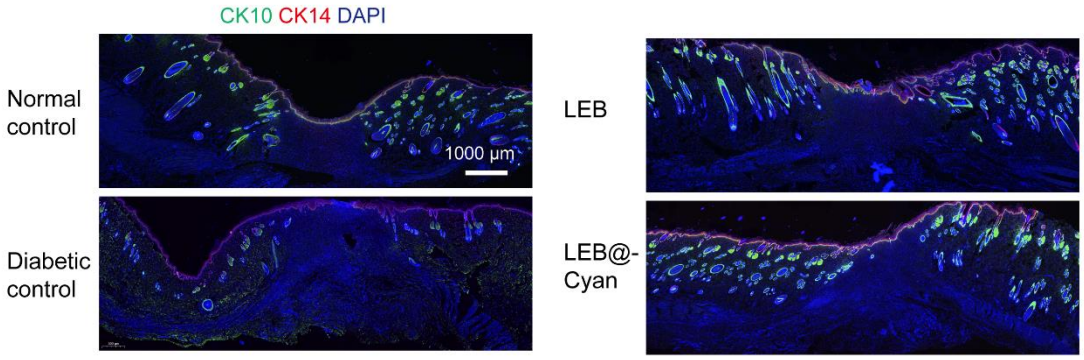

Figure S11. CK10 and CK14 immunofluorescence images of wound tissues of rats from different groups.

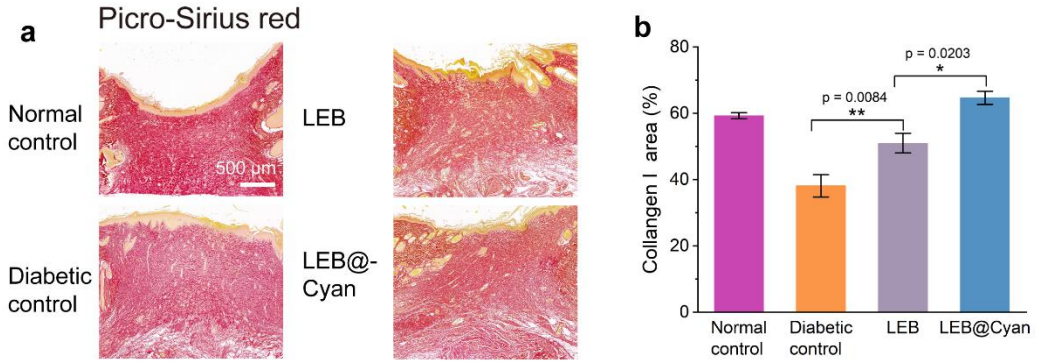

Figure S12. Representative images and quantification of Picro-Sirius red staining of wound tissues of rats from different groups. Data are expressed as means ± SD (N = 3). Statistical significances were calculated via Student's t-test. *P<0.05, **P<0.01.

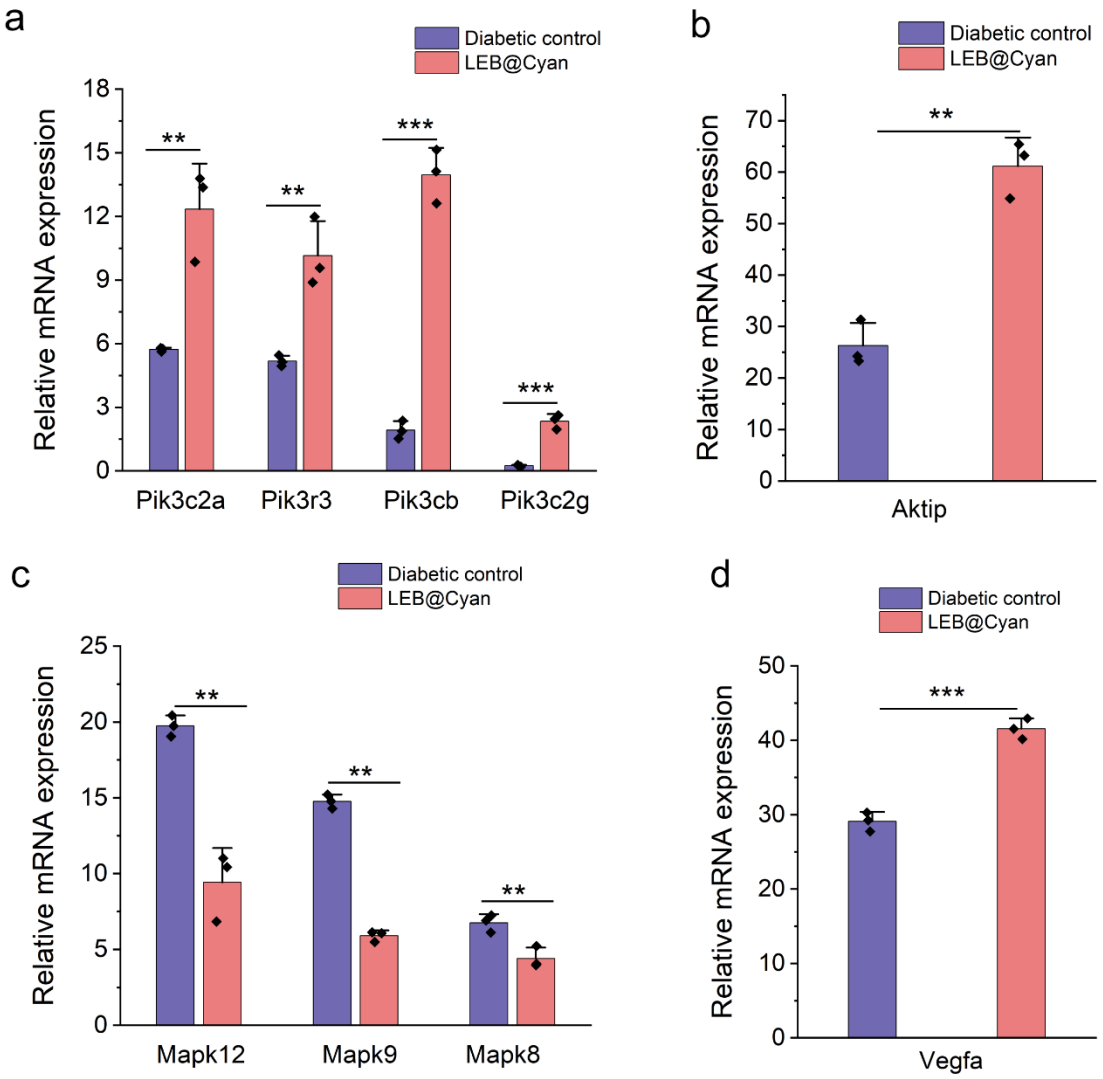

Figure S13. Relative mRNA expression of PI3K-AKT and MAPK signaling pathway. Data are expressed as means ± SD (N = 3). Statistical significances were calculated via Student's t-test. **P<0.01, ***P<0.001.

3. Supplementary Table

Table 1. LLLT for the diagnosis and treatment of the wound healing

Types of light sources	Therapeutic strategy	PBM specifications	Experimental models	Salient outcomes	Reference
Point light source	LLLT (Laser) + dendrosomal nanocurcumin (0.5 and 0.75 μM)	450 nm, 75 mW, 0.63 J/cm2 (224 s) or 0.95 J/cm2 (337 s)	Mouse embryonic fibroblast	Increased cell proliferation and migration; increased TGF-β and VEGF; decreased TNF-α and IL-6	[16]
Point light source	LLLT (Laser) + guarana (Paullinia cupana) extract	660 nm, 35 mW, 16 Hz, 4 J/cm2, 14 s	HFF-1 human dermal fibroblast	Increased IL-10 gene and protein expression; decerased pro-inflammatory molecules; FGF-1 and KGF-1	[17]
Point light source	LLLT (Laser) + silver nanoparticles (12 μg/mL)	104 mW, 830 nm, 5 J/cm2, 7 min and 16 s	WS1 human skin fibroblast	Increased cell migration and wound closure rate in normal	[18]

				wounded and diabetic wounded fibroblasts	
Point light source	LLLT (Laser) + tetrakis (4-carboxyphenyl) porphyrin and magnesium oxide nanoparticles (2 mg/mL)	635 nm, 45 J/cm2	L929 mouse fibroblast	Increased fibroblast viability; increased gene expressions of fibronectin 1, Col1α1, and vinculin	[19]
Flexible plane light source	LLLT (Multi-LED array) + dopamine-crosslinked hyaluronic acid/gelatin	630 nm, 4.59 mW/cm2	NIH/3T3 cells, wound rat model	Increased cell proliferation	[20]
Flexible plane light source	LLLT (Optical fiber-embedded fabric and laser) + rhodamine B	515 nm	————	pH assessment, photonic smart bandage	[21]